



ELSEVIER

Available online at www.sciencedirect.com

SCIENCE @ DIRECT®

Physica D 190 (2004) 15–37

PHYSICA D

www.elsevier.com/locate/physd

Monodromy in the resonant swing spring

Holger Dullin^{a,b,*}, Andrea Giacobbe^c, Richard Cushman^c

^a *Mathematical Sciences, Loughborough University, Loughborough LE11 3TU, UK*

^b *Institut für Theoretische Physik, Universität Bremen, 28334 Bremen, Germany*

^c *Mathematics Institute, University of Utrecht, 3508 TA Utrecht, The Netherlands*

Received 22 December 2002; received in revised form 24 September 2003; accepted 14 October 2003

Communicated by C.K.R.T. Jones

Abstract

In this paper, it is shown that an integrable approximation of the spring pendulum, when tuned to be in 1:1:2 resonance, has monodromy. The stepwise precession angle of the swing plane of the resonant spring pendulum is shown to be a rotation number of the integrable approximation. Due to the monodromy, this rotation number is not a globally defined function of the integrals. In fact at lowest order it is given by $\arg(\chi + i\lambda)$, where χ and λ are functions of the integrals. The resonant swing spring is therefore a system where monodromy has easily observed physical consequences.

© 2003 Elsevier B.V. All rights reserved.

PACS: 03.20.+i

Keywords: Monodromy; Spring pendulum; Resonance; Rotation number

1. Introduction

The spring pendulum, or swing spring, is one of the simplest possible mechanical systems. It is a spring with one end fixed, a mass attached at the other end, and a constant vertical gravitation field acting upon it. The name swing spring comes from the fact that, for appropriate initial conditions, the mass can either swing like a pendulum or bounce up and down like a spring. However, if in linear approximation near the equilibrium, the frequencies of the swinging and springing motion are in resonance, then these two types of motions are intricately intertwined. In particular, the following motion is easily observed: starting with a weakly unstable vertical springing motion, the system evolves into a planar swinging motion. This swinging motion is transient and the system returns to its original springing motion. This cycle then repeats. Lynch [6] observed that the orientation of the swing plane typically changes from one swinging phase to the next. Moreover, the angle between the swing planes of any two successive swinging phases is constant. However, the angle between the swing planes depends on initial conditions. He called this phenomenon the stepwise precession of the swing plane of the swing spring. It is this phenomenon that we are going to explain both qualitatively and quantitatively.

* Corresponding author. Tel.: +49-421-2182341; fax: +49-421-2184869.
E-mail address: h.r.dullin@lboro.ac.uk (H. Dullin).

The swing spring has a long history that is well described in [7]. The earliest comprehensive work on the planar spring pendulum is [12]. This paper gives a classical treatment of the 1:2 resonance using action-angle variables. It is written in the spirit of the old quantum mechanics and was actually motivated by the Fermi 1:2 resonance in CO₂. The advent of modern quantum mechanics seems to have made this type of analysis old-fashioned if not forgotten. As Lynch [7] points out most of the previous work is only concerned with the planar spring pendulum, so that the stepwise precession of the swing plane cannot be found in the old literature. Some progress on the three-dimensional system was made in [6]. After that Holm and Lynch [5] found that the system can be approximated by the 3-wave system and derived a differential equation for the angle of the swing plane. This was done using “pattern evocation in shape space” [8]. We show that the equation found by Holm and Lynch is exact and is nothing but the equation for the evolution of one of the angles of the action-angle coordinates of an integrable approximation to the resonant swing spring. We then trace the origin of the stepwise precession to the existence of Hamiltonian monodromy in this integrable approximation.

Hamiltonian monodromy is an obstruction to the existence of global action variables, which was first described in [3] (see also [2]). It generically appears around an equilibrium point of an integrable two degree of freedom Hamiltonian system whose linearization has a complex quartuple of eigenvalues [9,13]. Such an equilibrium point is called a focus–focus point. The integrable approximation of the resonant swing spring has three degrees of freedom. But after reduction of a symmetry, one obtains a two degree of freedom system with a focus–focus point as a relative equilibrium. Physically, this equilibrium corresponds to the pure springing motion of the system.

For the purpose of the present paper the most important consequence of monodromy is that the rotation number of invariant tori, that is, the ratio of their frequencies, near the singularity is not a single valued function. Our main result is that the stepwise precession of the swing plane is given by such a rotation number W , which explicitly has the form:

$$2\pi W = \arg(\chi + i\lambda) + O(\sqrt{\chi^2 + \lambda^2}). \quad (1)$$

Here χ is a scaled nonlinear energy and λ a scaled angular momentum. Hence both are simple functions of the integrals of the system, and $\chi, \lambda \rightarrow 0$ near the equilibrium of the swing spring. The amazing feature of (1) is that it is multi-valued and thus not differentiable at the origin. The multi-valuedness means that no matter how small the initial perturbation from the equilibrium is, one can always obtain all possible values for W . In general, such multi-valuedness has been described for integrable foliations near focus–focus points by Vũ Ngọc [11]. In some sense our result is a special case of his. However, he did not study the influence of the Hamiltonian, but only the foliation.

The paper is organized as follows. We briefly recall the physics of the swing spring in Section 2, and some basic facts about the harmonic oscillator in Section 3. Then we derive an integrable approximation in Section 4 which is valid near the resonant equilibrium point. This integrable system is reduced to a one degree of freedom system in Section 5, and the geometry of its energy momentum map is described in Section 6. The dynamics of the swing angle ϑ is analyzed in Section 7. In Section 8 we show that there is monodromy. Finally we obtain Eq. (1) for the rotation number W , by approximating an elliptic integral in Section 9.

2. The physics of the swing spring

The spring pendulum is a point particle $r = (x, y, z)$ in \mathbb{R}^3 of mass m attached to a spring which moves in a constant vertical gravitation field. Its potential energy is

$$\tilde{V}(r) = mgz + \frac{1}{2}k(\ell_0 - \|r\|)^2, \quad (2)$$

where $\|r\| = \sqrt{x^2 + y^2 + z^2}$. The unstretched length of the spring with spring constant k is ℓ_0 and g is the constant of gravity. The motion of the swing spring is governed by Newton's equations:

$$m\ddot{r} = -\text{grad } \tilde{V}(r). \quad (3)$$

The system is in equilibrium when the forces of gravity and the spring balance, that is, when

$$\text{grad } \tilde{V}(r) = 0. \quad (4)$$

Thus $x = y = 0$ and $z = -\ell$, where ℓ , the equilibrium length of the spring, is determined by

$$k(\ell - \ell_0) = mg. \quad (5)$$

Measuring length in units of equilibrium length ℓ , mass in units of m and time in units of $\sqrt{g/\ell}$ (which is the period of small amplitude pendulum oscillations), we see that the Hamiltonian of the swing spring on phase space $T^*\mathbb{R}^3$ with canonical coordinates $Z = (x, y, z, p_x, p_y, p_z)$ is

$$\tilde{H}(Z) = \frac{1}{2}(p_x^2 + p_y^2 + p_z^2) + \tilde{V}(x, y, z), \quad (6)$$

where

$$\tilde{V}(x, y, z) = z + \frac{1}{2}v^2 \left(1 - \frac{1}{v^2} - \sqrt{x^2 + y^2 + z^2}\right)^2 \quad (7)$$

and $v = \sqrt{k\ell/mg} = \sqrt{\ell/(\ell - \ell_0)}$. Since $\ell > \ell_0$, we have $v > 1$. This implies that the frequency of the spring oscillation is greater than the frequency of the small amplitude pendulum oscillations. The reason for this is that these frequencies are *not* independent because they are coupled by (5).

The Hamiltonian \tilde{H} is invariant under rotation about the z -axis. This implies that the angular momentum:

$$L = xp_y - yp_x \quad (8)$$

is a constant of motion. A third integral of the Hamiltonian system $(\tilde{H}, T^*\mathbb{R}^3)$ is not known and numerical experiments indicate that it is nonintegrable. As a first step in our analysis, we derive an approximating integrable system by averaging near the elliptic equilibrium.

Expanding the potential \tilde{V} (7) about its minimum $(0, 0, -1)$ to cubic terms gives

$$V_2 + V_3 = \frac{1}{2}(x^2 + y^2 + v^2z^2) - \tilde{\mu}(x^2 + y^2)z, \quad (9)$$

where z from now on is the displacement from -1 and $\tilde{\mu} = (1/2)(v^2 - 1) \geq 0$. Thus the quadratic approximation to the Hamiltonian of the swing spring in dimensionless variables with its equilibrium shifted to the origin is

$$H_2 = \frac{1}{2}(p_x^2 + p_y^2 + p_z^2) + \frac{1}{2}(x^2 + y^2 + v^2z^2). \quad (10)$$

For a generic (irrational) choice of the constant v , the frequencies of small oscillations of (10) near the stable equilibrium are not in full resonance. When the physical constants are chosen so that the frequencies are in 1:1:2 resonance (corresponding to $v = 2$), then the system evolves in accordance with the description in Section 1, and thus shows the phenomenon of energy exchange and of precession of the swing plane. In the remainder of this paper, we will concentrate exclusively on the 1:1:2 resonant case $v = 2$. When $v \neq 2$ an oscillation on the z -axis with sufficiently small amplitude is stable, and undergoes a Hamiltonian Hopf bifurcation for increasing amplitude. This will be shown in a forthcoming paper using Floquet theory and Hill's determinant. This case is analyzed as an example in [4] using normal form theory.

3. Prelude: the 1:1 resonance

In order to understand the swing plane angle and to motivate a coordinate change needed in the following sections, we recall some facts about the isotropic harmonic oscillator with two degrees of freedom. Its Hamiltonian is the xy -part of H_2 (10), namely,

$$H_{xy} = \frac{1}{2}(p_x^2 + p_y^2 + x^2 + y^2). \quad (11)$$

The Hamiltonian H_{xy} is an action, because it has a periodic flow with minimal period 2π for every initial condition with positive energy.¹ The system (11) is superintegrable: it has more integrals than degrees of freedom. They are the individual energies of the oscillators $H_x = (1/2)(p_x^2 + x^2)$, $H_y = (1/2)(p_y^2 + y^2)$, angular momentum $L = xp_y - yp_x$, and $M = xy + p_x p_y$. In fact, these four polynomial invariants generate the algebra of all polynomials which are invariant under the flow of $X_{H_{xy}}$, see [2]. They are not independent but satisfy the relation $4H_x H_y = L^2 + M^2$, which defines a curve in the energy surface $\{H_{xy} = h_{xy}\}$. Here and in the following, we use the convention that a small letter denotes the value of the conserved quantity of the corresponding capital letter, so that for example $\{L = xp_y - yp_x = l\}$ defines a hypersurface in phase space of constant angular momentum l .² The energy surface has the topology of S^3 , and the orbits of H_{xy} define the Hopf fibration of S^3 . The space of orbits is obtained as the quotient of S^3 by the Hamiltonian flow. This quotient space is a sphere $S^2 = S^3/S^1$. The Hopf map from the energy surface S^3 onto the sphere S^2 is given by $(L, M, H_x - H_y)$. This latter sphere of radius h_{xy} is embedded in \mathbb{R}^3 with coordinates $L, M, H_x - H_y$, namely

$$L^2 + M^2 + (H_x - H_y)^2 = (H_x + H_y)^2 = h_{xy}^2. \quad (12)$$

In phase space all the periodic orbits of a fixed energy h_{xy} are parameterized by this S^2 . When considering their projection from phase space onto configuration space they are oriented ellipses with different eccentricity and spatial orientation. The angular momentum L (8) determines the area of the ellipse. An angle ϑ conjugate to L determines the line on which the major axis lies.

In a superintegrable system there exist generalized action-angle coordinates in the sense of Nehorošev [10] which we are now going to construct. The single dynamically relevant action is the Hamiltonian itself. An angle α conjugate to H_{xy} satisfies $\{\alpha, H_{xy}\} = 1$. The other two coordinates give a parameterization of the twice punctured sphere S^2 and α must be chosen so to commute with them.³ As coordinates on the twice punctured S^2 we choose L and a conjugate angle ϑ . The choice of L is somewhat arbitrary at this point, but (1) L has a clear geometric meaning for the projection of the orbits onto configuration space, and (2) as we already noted for the swing spring L is a constant of motion (unlike the other three invariants). This is typical in superintegrable systems, namely, the form of the perturbation distinguishes one of the separating coordinate systems.

To find a generalized action-angle coordinate system we first perform a linear symplectic change of coordinates that simultaneously diagonalizes H_{xy} and L . Since the Hessian of H_{xy} is the identity, it is diagonal in any coordinate system. The Hessian of L has eigenvalues ± 1 with multiplicity 2 each. Up to permutation and a rotation in each eigenspace (which amounts to a choice of phase of the conjugate angles) the desired transformation is given by

$$(x, y, p_x, p_y) = \frac{1}{\sqrt{2}}(\xi + p_\eta, \eta + p_\xi, p_\xi - \eta, p_\eta - \xi). \quad (13)$$

¹ From now on we assume that the energy is positive.

² Not to be confused with the spring length ℓ , which does not appear in the rest of this paper.

³ For example, $(1/2)(\arg(x - ip_x) + \arg(y - ip_y))$ is conjugate to H_{xy} , and therefore parameterizes the orbits, but it does not, e.g., commute with L .

In these coordinates L reads

$$L = \frac{1}{2}(p_\eta^2 + \eta^2) - \frac{1}{2}(p_\xi^2 + \xi^2)$$

and H_{xy} has the same form as before, see (11). Using the $(\xi, \eta, p_\xi, p_\eta)$ variables we obtain the following well known result, see Appendix A for a proof.

Lemma 1. *A system of generalized action-angle coordinates for the isotropic harmonic oscillator (11) is given by the action H_{xy} with conjugate angle:*

$$\alpha = \frac{1}{2}(\arg(\eta - ip_\eta) + \arg(\xi - ip_\xi)) \quad (14)$$

and by the symplectic coordinates (L, ϑ) on the orbit space S^2 minus two points where

$$\vartheta = \frac{1}{2} \left(\frac{\pi}{2} + \arg(\eta - ip_\eta) - \arg(\xi - ip_\xi) \right). \quad (15)$$

The orbit space parameterizes the shape and orientation of the ellipse obtained by projection of an orbit of the harmonic oscillator vector field $X_{H_{xy}}$ onto configuration space. The line on which the major axis lies is given by ϑ , the angle between the x -axis and the major axis, and its area by πl^2 . Its eccentricity e is determined by h_{xy} and l from

$$e = 2(\kappa + \kappa^{-1})^{-1}, \quad \kappa^4 = \frac{h_{xy} - l}{h_{xy} + l}. \quad (16)$$

The above ‘coordinate system’ on S^2 is not defined when either $\xi = p_\xi = 0$ or $\eta = p_\eta = 0$, that is when either $h_{xy} = l$ or $h_{xy} = -l$, respectively. In these special cases, the projection of the orbit is a circle. Therefore the semimajor axis, and hence ϑ , is not defined. S^2 can therefore be understood as having an axis with accessible values $l \in [-h_{xy}, h_{xy}]$ where $l = 0$ is the equator and $l = \pm h_{xy}$ the north and south pole. For fixed latitude l the longitude ϑ gives the direction of the major axis of the ellipse whose shape is determined by l . Note that $\vartheta \in [-\pi/2, \pi/2]$ because it does not distinguish rays, but only lines. Therefore, technically speaking, ϑ lives in the one-dimensional projective space \mathbb{RP}^1 . This also explains why there is an additional factor of 2 when compared to the angle $\arg(H_x - H_y + iM)$.

The types of projections of the orbits of $X_{H_{xy}}$ fall into three cases:

1. $0 < |l| < h_{xy}$: elliptic motion,
2. $l = 0$: linear motion,
3. $l = \pm h_{xy}$: circular motion.

In the following sections, these three cases will reappear as part of the analysis of the 1:1:2 resonant swing spring. In that case however, neither the eccentricity nor the spatial orientation of the instantaneous ellipse will be constant, but will slowly vary with time, see Section 7.

The form of the angle variables suggests that the sum and difference of H_{xy} and L are good constants of motion. Similar constants of motion will be introduced in the next section.

4. An approximating integrable system

The first approximation to the Hamiltonian (6) of the swing spring is the truncation of its Taylor expansion at the equilibrium, namely, (10) with $\nu = 2$. The Hamiltonian of the resonant swing spring in its cubic approximation is

$$\hat{H} = H_2 + V_3 = \frac{1}{2}(p_x^2 + p_y^2 + p_z^2) + \frac{1}{2}(x^2 + y^2 + 4z^2) - \tilde{\mu}(x^2 + y^2)z. \quad (17)$$

By rescaling the coordinates and changing the time scale, we may consider $\tilde{\mu}$ to be a small parameter, which measures the distance to the origin.

The second approximation is the first order normal form of \hat{H} (17). In our case, the normal form is obtained by averaging over the flow of the quadratic part of \hat{H} . Due to the resonance there will be secular terms at cubic order. From general results it is known that a large measure of initial conditions of the averaged system stays close to the original solutions for long times, see [1].

The quadratic terms H_2 of the Hamiltonian \hat{H} are a 1:1:2 resonator. The flow generated by H_2 is

$$\psi : (t, Z) \mapsto \psi_t(Z) = \left(\begin{array}{ccc|ccc} \cos t & 0 & 0 & \sin t & 0 & 0 \\ 0 & \cos t & 0 & 0 & \sin t & 0 \\ 0 & 0 & \cos 2t & 0 & 0 & \frac{1}{2} \sin 2t \\ \hline -\sin t & 0 & 0 & \cos t & 0 & 0 \\ 0 & -\sin t & 0 & 0 & \cos t & 0 \\ 0 & 0 & -2 \sin 2t & 0 & 0 & \cos 2t \end{array} \right) Z, \quad (18)$$

where $Z = (x, y, z, p_x, p_y, p_z)$.

The normal form of the Hamiltonian \hat{H} is obtained by averaging over the flow of H_2 , and is

$$H(Z) = \frac{1}{2\pi} \int_0^{2\pi} \hat{H} \circ \psi_t(Z) dt = H_2 - \frac{\tilde{\mu}}{8} [(xp_x + yp_y)p_z + (x^2 + y^2)z - (p_x^2 + p_y^2)z]. \quad (19)$$

By construction the new Hamiltonian H (19) is invariant under S^1 symmetry (18), that is, $\{H, H_2\} = 0$, where $\{, \}$ is the standard Poisson bracket corresponding to $\omega = dx \wedge dp_x + dy \wedge dp_y + dz \wedge dp_z$. It is straightforward to check that H also commutes with the angular momentum L . Since the two symmetries generated by H_2 and L commute, $\{H_2, L\} = 0$ and are almost everywhere independent, it follows that the system $(H, H_2, L, T^*\mathbb{R}^3, \omega)$ is Liouville integrable.

Now we introduce new canonical coordinates \mathcal{E} that diagonalize both, H_2 and L . As these have been discussed in detail in Section 3, here we merely extend this transformation by a scaling in z and p_z . The new variables are given by the linear symplectic map:

$$\mathcal{E} = (\xi, \eta, \zeta, p_\xi, p_\eta, p_\zeta) = \frac{1}{\sqrt{2}}(x - p_y, y - p_x, 2z, p_x + y, p_y + x, p_z). \quad (20)$$

In the new coordinates we obtain

$$L = \frac{1}{2}(p_\eta^2 + \eta^2) - \frac{1}{2}(p_\xi^2 + \xi^2), \quad (21a)$$

$$H_2 = \frac{1}{2}(p_\xi^2 + \xi^2 + p_\eta^2 + \eta^2 + 2(p_\zeta^2 + \zeta^2)), \quad (21b)$$

$$H = H_2 + \mu[(\xi p_\zeta - \zeta p_\xi)\eta - (\xi\zeta + p_\xi p_\zeta)p_\eta], \quad (21c)$$

where $\mu = \sqrt{2}\tilde{\mu}/8 = 3\sqrt{2}/16$. Hamilton's equations in the \mathcal{E} coordinates are

$$\begin{aligned} \dot{\xi} &= p_\xi - \mu(\eta\zeta + p_\eta p_\zeta), & \dot{p}_\xi &= -\xi - \mu(\eta p_\zeta - \zeta p_\eta), & \dot{\eta} &= p_\eta - \mu(\xi\zeta + p_\xi p_\zeta), \\ \dot{p}_\eta &= -\eta - \mu(\xi p_\zeta - \zeta p_\xi), & \dot{\zeta} &= 2p_\zeta + \mu(\xi\eta - p_\xi p_\eta), & \dot{p}_\zeta &= -2\zeta + \mu(\xi p_\eta + \eta p_\xi). \end{aligned} \quad (22)$$

This is a variant of the 3-wave system, see [5] and the references therein. The crucial difference of (22) with the usual presentation of the 3-wave system is that we retain the linear terms. These terms usually are removed by the ansatz $\xi + ip_\xi = A \exp(it)$, etc., which leads to equations in the amplitudes A etc., see [5]. In our treatment we retain the linear terms, because they determine the swing plane to lowest order. Keeping these terms enables us to find the swing plane *without* invoking the ‘‘pattern evocation in shape space’’ hypothesis, as was done in [5].

5. Reduction to one degree of freedom

The truncated averaged resonant swing spring $(H, T^*\mathbb{R}^3)$ is Liouville integrable, and has two S^1 symmetries. In the classical approach, a “coordinate system” is introduced that has the corresponding conserved quantities as momenta, together with conjugate angles. This is very efficient, but this “coordinate system” has a singularity exactly at the pure springing motion we want to study. This is why we use singular reduction [2] in order to obtain a one degree of freedom system that properly describes the motion close to pure springing motion. Towards this goal, we introduce slightly simpler momenta J_1, J_2 in place of H_2, L . We then reduce the system by the effective two-torus action generated by the momenta J_1 and J_2 .

The new momenta are given by

$$J_1 = \frac{1}{2}(H_2 - L) = \frac{1}{2}(p_\xi^2 + \xi^2 + p_\zeta^2 + \zeta^2), \quad (23a)$$

$$J_2 = \frac{1}{2}(H_2 + L) = \frac{1}{2}(p_\eta^2 + \eta^2 + p_\zeta^2 + \zeta^2), \quad (23b)$$

whose Hamiltonian vectors fields X_{J_1} and X_{J_2} have flows giving the S^1 -actions:

$$\phi_t^{J_1} : (t, \Xi) \mapsto \left(\begin{array}{ccc|ccc} \cos t & 0 & 0 & \sin t & 0 & 0 \\ 0 & 1 & 0 & 0 & 0 & 0 \\ 0 & 0 & \cos t & 0 & 0 & \sin t \\ \hline -\sin t & 0 & 0 & \cos t & 0 & 0 \\ 0 & 0 & 0 & 0 & 1 & 0 \\ 0 & 0 & -\sin t & 0 & 0 & \cos t \end{array} \right) \Xi, \quad (24a)$$

$$\phi_s^{J_2} : (s, \Xi) \mapsto \left(\begin{array}{ccc|ccc} 1 & 0 & 0 & 0 & 0 & 0 \\ 0 & \cos s & 0 & 0 & \sin s & 0 \\ 0 & 0 & \cos s & 0 & 0 & \sin s \\ \hline 0 & 0 & 0 & 1 & 0 & 0 \\ 0 & -\sin s & 0 & 0 & \cos s & 0 \\ 0 & 0 & -\sin s & 0 & 0 & \cos s \end{array} \right) \Xi, \quad (24b)$$

respectively. Here $\mathcal{E} = (\xi, \eta, \zeta, p_\xi, p_\eta, p_\zeta)$. These S^1 -actions commute and leave the Hamiltonian (21c) invariant. Thus $(H, J_1, J_2, T^*\mathbb{R}^3, \omega)$ is a Liouville integrable system. For most of the analysis, we will use this set of constants of motion and the coordinates \mathcal{E} . For the physical interpretation it is sometimes better to use the coordinates Z and the constants H_2 and L .

Now define a T^2 -action

$$\begin{aligned} \Phi : T^2 \times T^*\mathbb{R}^3 &\rightarrow T^*\mathbb{R}^3, \\ ((t, s), \Xi) &\mapsto \phi_t^{J_1} \circ \phi_s^{J_2}(\Xi) = \left(\begin{array}{ccc|ccc} \cos t & 0 & 0 & \sin t & 0 & 0 \\ 0 & \cos s & 0 & 0 & \sin s & 0 \\ 0 & 0 & \cos(t+s) & 0 & 0 & \sin(t+s) \\ \hline -\sin t & 0 & 0 & \cos t & 0 & 0 \\ 0 & -\sin s & 0 & 0 & \cos s & 0 \\ 0 & 0 & -\sin(t+s) & 0 & 0 & \cos(t+s) \end{array} \right) \Xi, \end{aligned} \quad (25)$$

which comes from composing the commuting circle actions (24a) and (24b). The momentum mapping of this two-torus action⁴ is the map:

$$\mathcal{J} : T^*\mathbb{R}^3 \rightarrow \mathbb{R}^2 : \mathcal{E} \mapsto (J_1(\mathcal{E}), J_2(\mathcal{E})). \quad (26)$$

To reduce the integrable system $(H, J_1, J_2, T^*\mathbb{R}^3, \omega)$ by the symmetry Φ , we use invariant theory. Let the symmetry Φ act on polynomials in the six variables \mathcal{E} . A subset of polynomials will be invariant under Φ . These invariant polynomials form an algebra. By the Hilbert basis theorem this algebra is generated by a finite set of invariant polynomials, that is, every invariant polynomial can be written as a polynomial in the generating polynomials. The reduction with respect to the symmetry group action Φ is achieved by taking these generators as new coordinates.

⁴ To distinguish a physical action (that is, a constant of motion which generates a periodic flow) from an action of a Lie group G , we will always call the latter a G -action.

In particular the Hamiltonian and the constants of motion can all be written in terms of these coordinates. In our case the algebra of Φ -invariant polynomials is generated by

$$\rho_1 = p_\xi^2 + \xi^2, \quad \rho_2 = p_\eta^2 + \eta^2, \quad \rho_3 = p_\zeta^2 + \zeta^2 \quad (27)$$

and

$$\rho_4 = (\xi\eta - p_\xi p_\eta)p_\zeta - (\xi p_\eta + \eta p_\xi)\zeta, \quad \rho_5 = (\xi\eta - p_\xi p_\eta)\zeta + (\xi p_\eta + \eta p_\xi)p_\zeta. \quad (28)$$

The invariance of ρ_4 and ρ_5 is more obvious if we write Φ in complex coordinates $z_1 = \xi + ip_\xi$, $z_2 = \eta + ip_\eta$, $z_3 = \zeta + ip_\zeta$ and note that

$$\rho_5 + i\rho_4 = \bar{z}_1 \bar{z}_2 z_3 = (\xi - ip_\xi)(\eta - ip_\eta)(\zeta + ip_\zeta).$$

To show that ρ_i are a basis of the algebra of invariant polynomials it is enough to show that every invariant monomial can be written in terms of them. This can be done in complex coordinates, because in these coordinates the Φ -invariant monomials can easily be written down.

The Hamiltonian H (21c) and conserved momenta J_i when expressed in terms of the generating polynomials are

$$H = \frac{1}{2}(\rho_1 + \rho_2 + 2\rho_3) + \mu\rho_4, \quad (29a)$$

$$J_1 = \frac{1}{2}(\rho_1 + \rho_3), \quad (29b)$$

$$J_2 = \frac{1}{2}(\rho_2 + \rho_3). \quad (29c)$$

The invariants (27) and (28) are not independent, but are subject to the relation:

$$\rho_4^2 + \rho_5^2 = \rho_1\rho_2\rho_3, \quad \rho_1 \geq 0, \quad \rho_2 \geq 0, \quad \rho_3 \geq 0. \quad (30)$$

Now we want to fix the values of the conserved momenta, and study the remaining one degree of freedom motion. Fixing $(J_1, J_2) = (j_1, j_2)$ means that we consider the (j_1, j_2) -level set of the momentum map \mathcal{J} (26) in phase space. Not only do we fix the momenta, but in carrying out singular reduction we also remove the dynamics that is generated by \mathcal{J} . This means that the reduced phase space P_{j_1, j_2} (which is possibly singular) is the space of orbits of the symmetry group action Φ with momentum (j_1, j_2) : formally, $P_{j_1, j_2} = \mathcal{J}^{-1}(j_1, j_2)/T^2$. This set is defined by (30) together with

$$\rho_1 + \rho_3 = 2j_1, \quad \rho_2 + \rho_3 = 2j_2, \quad (31)$$

which come from (29b) and (29c). Using (31) ρ_1 and ρ_2 can be eliminated from (30). The defining equation of P_{j_1, j_2} is then

$$G_{j_1, j_2}(\rho_3, \rho_4, \rho_5) = \rho_4^2 + \rho_5^2 - \rho_3(2j_1 - \rho_3)(2j_2 - \rho_3) = 0, \quad (32)$$

where $0 \leq \rho_3 \leq \min(2j_1, 2j_2)$. Hence P_{j_1, j_2} is a semialgebraic variety in \mathbb{R}^3 with coordinates (ρ_3, ρ_4, ρ_5) . Because both ρ_3 and $\rho_4^2 + \rho_5^2$ are nonnegative, there are three nontrivial possibilities for the geometry of P_{j_1, j_2} , see Fig. 1. These possibilities are determined by the position of the roots of the polynomial:

$$P_3(\rho_3) = \rho_3(2j_1 - \rho_3)(2j_2 - \rho_3). \quad (33)$$

The reduced phase space P_{j_1, j_2} (32) can have three different topologies:

1. $j_1 \neq j_2 \neq 0$. The space $\mathcal{J}^{-1}(j_1, j_2)$ is smooth and the action Φ (25) is free. The reduced space is diffeomorphic to a smooth 2-sphere, see Fig. 1 left. The dynamics generated by \mathcal{J} in full phase space is a two-torus for every initial point in P_{j_1, j_2} . In other words, every point in the reduced space reconstructs to a two-torus orbit of the free action Φ in phase space.

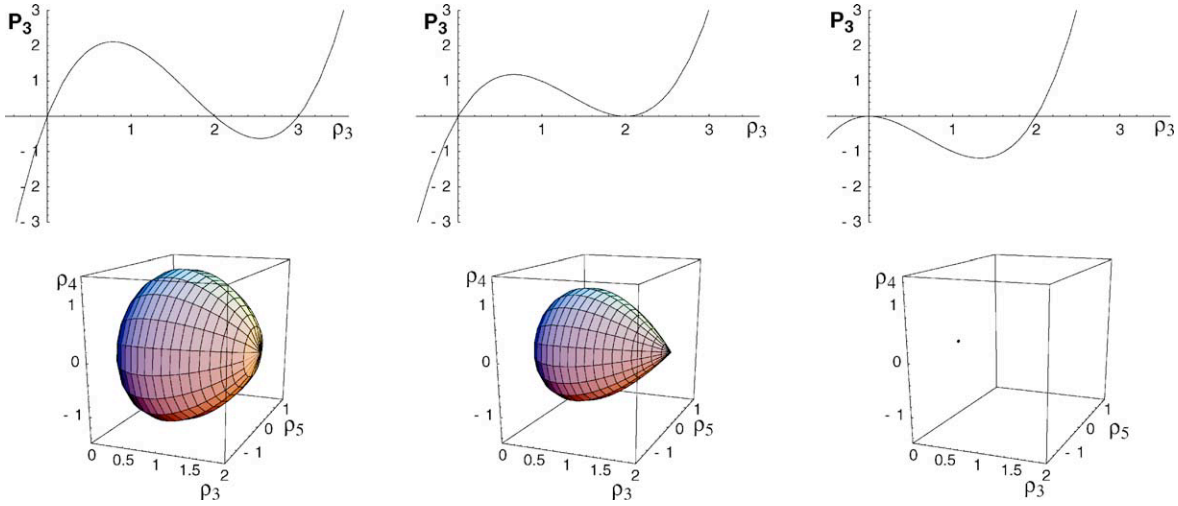


Fig. 1. The polynomial P_3 (upper row) and the corresponding reduced spaces P_{j_1, j_2} (lower row) illustrating the three types of reduced space: (1) $j_1 = 1 < j_2 = 3/2$ (left); (2) $j_1 = j_2 = 1$ (middle); and (3) $j_1 = 0, j_2 = 1$ (right).

2. $j_1 = j_2 \neq 0$. The space $\mathcal{J}^{-1}(j_1, j_1)$ is smooth and the action Φ has a fixed point $(\rho_3, \rho_4, \rho_5, \rho_3) = (2j_1, 0, 0)$ with isotropy group S^1 . Then the reduced space is a “turnip”, that is, a *topological* 2-sphere with one (conical) singular point $(0, 0, 2j_1)$, see Fig. 1 middle. This singular point reconstructs to a pure springing motion on $\xi = \eta = p_\xi = p_\eta = 0$ and $\zeta^2 + p_\zeta^2 = 2j_1$. All other points of the reduced space reconstruct to a two-torus in phase space which has angular momentum L equal to zero. This two-torus dynamically decomposes into an S^1 family of planar motions.
3. $j_1 = 0 < j_2$ or $j_2 = 0 < j_1$. Each of the reduced spaces $P_{j_1, 0}$ and P_{0, j_2} is the point $\rho_4 = \rho_5 = \rho_3 = 0$, see Fig. 1 right. In $T^*\mathbb{R}^3$ each point corresponds to a pure swinging motion with nonzero angular momentum L on the circle $\xi^2 + p_\xi^2 = 2j_1, \eta = p_\eta = \zeta = p_\zeta = 0$ (counterclockwise in the (x, y) -plane projection) or the circle $\eta^2 + p_\eta^2 = 2j_2, \xi = p_\xi = \zeta = p_\zeta = 0$ (clockwise), respectively. In the particular case $j_1 = j_2 = 0$, the reduced space $P_{0, 0}$ again is the point $\rho_4 = \rho_5 = \rho_3 = 0$, which this time reconstructs to the equilibrium point $\xi = p_\xi = \eta = p_\eta = \zeta = p_\zeta = 0$.

Since the Hamiltonian H (21c) is invariant under the T^2 action Φ (25), it induces a Hamiltonian function on the reduced space given by

$$H_{j_1, j_2} : P_{j_1, j_2} \subseteq \mathbb{R}^3 \rightarrow \mathbb{R} : (\rho_3, \rho_4, \rho_5) \mapsto j_1 + j_2 + \mu\rho_4. \quad (34)$$

The integral curves of the reduced one degree of freedom system are the intersection of the reduced phase space P_{j_1, j_2} and the planes $\{H_{j_1, j_2} = h\}$, as illustrated in Fig. 2. The fact that the Hamiltonian is a linear function does *not* imply that the system is a linear dynamical system, because the nonlinearity is contained in the Poisson bracket that gives the dynamics on the reduced space. The original Poisson bracket on $T^*\mathbb{R}^3$ induces a Poisson bracket on the reduced space \mathbb{R}^5 with coordinates (ρ_1, \dots, ρ_5) . The reduced brackets are simply obtained by calculating the brackets in the original variables, and then re-expressing them in terms of the generators of the invariants. This is always possible, because the bracket of invariant polynomials is again an invariant polynomial. We obtain the following nonzero brackets:

$$\begin{aligned} \{\rho_1, \rho_4\} = \{\rho_2, \rho_4\} = \{\rho_4, \rho_3\} = -2\rho_5, & \quad \{\rho_1, \rho_5\} = \{\rho_2, \rho_5\} = \{\rho_5, \rho_3\} = 2\rho_4, \\ \{\rho_4, \rho_5\} = (\rho_1 + \rho_2)\rho_3 - \rho_1\rho_2. & \end{aligned} \quad (35)$$

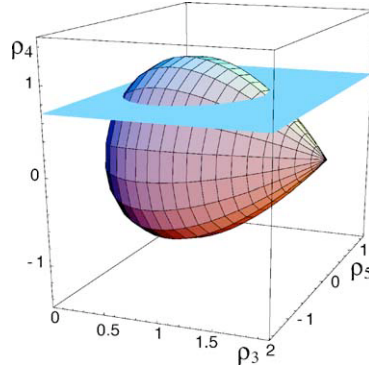


Fig. 2. The intersection of the singular reduced space $P_{1,1}$ with the plane $h = \text{const.}$ gives an integral curve of the reduced one degree of freedom system.

By direct computation it is easy to check that the above brackets satisfy the Jacobi identity. Since we have removed the dynamics generated by the components of \mathcal{J} to obtain the reduced dynamics, the generators (29b) and (29c) are Casimirs for the Poisson algebra on the reduced space. They are used to eliminate ρ_1 and ρ_2 , which gives a Poisson bracket on \mathbb{R}^3 (with coordinates (ρ_3, ρ_4, ρ_5)) given by

$$\{\rho_3, \rho_4\} = 2\rho_5, \quad \{\rho_4, \rho_5\} = 2\rho_3(j_1 + j_2 - \rho_3) - (2j_1 - \rho_3)(2j_2 - \rho_3), \quad \{\rho_5, \rho_3\} = 2\rho_4. \quad (36)$$

This bracket has the relation (30) as a Casimir. So the reduced phase space P_{j_1, j_2} is a symplectic leaf of the reduced Poisson bracket. Hence the vector field of the reduce Hamiltonian H_{j_1, j_2} on the reduced phase space P_{j_1, j_2} is given by

$$\dot{\rho}_4 = \{\rho_4, H_{j_1, j_2}\} = 0, \quad \dot{\rho}_5 = \{\rho_5, H_{j_1, j_2}\} = \mu P'_3(\rho_3), \quad \dot{\rho}_3 = \{\rho_3, H_{j_1, j_2}\} = 2\mu\rho_5. \quad (37)$$

Combining the last two equations in (37) we arrive at a single second order equation:

$$\ddot{\rho}_3 = 2\mu^2 P'_3(\rho_3) \quad (38)$$

that gives the reduced dynamics, where the “potential” P_3 is given by (33). The differential equation (38) describes the evolution of the square of the amplitude of z -oscillation (recall that $\rho_3 = (1/2)(p_z^2 + 4z^2)$ in original variables). Eq. (38) can be integrated to

$$\dot{\rho}_3^2 = 4\mu^2 P_3(\rho_3) - c. \quad (39)$$

We will see later that the integration constant $c = 4(h - j_1 - j_2)^2$.

When $j_1 = j_2 > 0$, the $h = 2j_1$ -level set of the reduced Hamiltonian H_{j_1, j_1} (34) is the intersection of the 2-plane $\{H_{j_1, j_1} = h\} = \{\rho_4 = 0\}$ with the reduced space P_{j_1, j_1} . This integral curve is homoclinic to the conical singular point $(2j_1, 0, 0)$ of P_{j_1, j_1} . The conical singular point reconstructs in phase space to the hyperbolic periodic orbit of pure springing motion; while the homoclinic loop reconstructs to a 2-torus bundle over each point of $H_{j_1, j_1}^{-1}(2j_1) \setminus \{(2j_1, 0, 0)\}$. Thus $H_{j_1, j_1}^{-1}(2j_1)$ reconstructs to the stable and unstable manifold of the hyperbolic periodic orbit. This invariant manifold is the product of a once pinched 2-torus and a circle. Describing the geometry of the 3-torus bundle and the dynamics of the swing spring near this homoclinic invariant manifold is the main objective of the remainder of this paper.

6. Critical values of the energy momentum map

The truncated and averaged swing spring $(H, T^*\mathbb{R}^3)$ is Liouville integrable and has three degrees of freedom. The Liouville–Arnold theorem implies that almost all initial conditions lead to dynamics on three-tori. At special points where the constants of motion are not independent, the motion takes place on a lower-dimensional space. An example of this occurs for relative equilibria in which only rotation about the z -axis takes place, or equilibria, with no motion at all. All this information is contained in the geometry of the energy momentum map:

$$\mathcal{EM} : T^*\mathbb{R}^3 \rightarrow \mathbb{R}^3 : \mathcal{E} \mapsto (H(\mathcal{E}), J_1(\mathcal{E}), J_2(\mathcal{E})) \quad (40)$$

of the Liouville integrable system $(H, J_1, J_2, T^*\mathbb{R}^3, \omega)$. In this section, we determine the set of critical values Σ of the energy momentum mapping (40). Knowing the image and critical values of the energy momentum map, we can use the information obtained in Section 5, to discuss the types of motion that correspond to the different critical values. The critical values of \mathcal{EM} are determined by the equilibrium points of the reduced system, because an equilibrium of the reduced system reconstructs to a lower-dimensional invariant set. Later we will see that the converse is also true. Geometrically, equilibrium points of the reduced system correspond to energies h for which the plane $\{H_{j_1, j_2} = h\}$ is either tangent to the reduced space P_{j_1, j_2} , or intersects it at a (singular) point. The roman numerals I, II and III refer to the equilibrium points found in the corresponding cases 1, 2 and 3 of Section 5, respectively:

- (I) $j_1 \neq j_2 \neq 0$: critical points always correspond to tangencies.
- (II) $j_1 = j_2 \neq 0$: critical points occur either because the plane $\{H_{j_1, j_1} = h\}$ contains the conical singular point $(\rho_3, \rho_4, \rho_5) = (2j_1, 0, 0)$ of the turnip (case IIa) or because of a tangency to a smooth part of the turnip (case IIb). The conical singular point corresponds to the critical value $(H, J_1, J_2) = (2j_1, j_1, j_1)$ of \mathcal{EM} .
- (III) $j_1 = 0$ or $j_2 = 0$: the critical values for which the plane $\{H_{j_1, j_2} = h\}$ contains the point P_{j_1, j_2} are $(j_1, j_1, 0)$ or $(j_2, 0, j_2)$, respectively.

The points of tangency between $\{H_{j_1, j_2} = h\}$ and P_{j_1, j_2} occur at extrema of H_{j_1, j_2} restricted to P_{j_1, j_2} . Therefore, they can be computed using Lagrange multipliers. Requiring the gradients of H_{j_1, j_2} (34) and G_{j_1, j_2} (32) with respect to (ρ_3, ρ_4, ρ_5) to be parallel gives $\rho_5 = 0$ and $P'_3(\rho_3) = 0$. Eliminating ρ_4 using the Hamiltonian gives

$$Q_3(\rho_3) = -G_{j_1, j_2} \left(\rho_3, \frac{h - j_1 - j_2}{\mu}, 0 \right) = \rho_3(2j_1 - \rho_3)(2j_2 - \rho_3) - \frac{(h - j_1 - j_2)^2}{\mu^2}. \quad (41)$$

Since $Q'_3 = P'_3 = 0$, tangencies occur at multiple roots of Q_3 . The discriminant surface of the polynomial Q_3 is the set of parameters (h, j_1, j_2) for which Q_3 has (possibly complex) multiple roots. Restricting to real roots in $[0, \min(2j_1, 2j_2)]$ one obtains the tangencies relevant for determining the points described in point I. In case II when $h = 2j_1$ then $\rho_3 = 2j_1$ is a double root of Q_3 at the boundary of $[0, 2j_1]$. In case III there is a double root at $\rho_3 = 0$, which degenerates into a triple root when $j_1 = j_2 = h = 0$. Hence the information needed to draw the set of critical values Σ are contained in the discriminant locus of Q_3 restricted to real roots in $[0, \min(2j_1, 2j_2)]$.

The following argument determines a parameterization of the set Σ by the position of the real double root $s \in [0, \min(2j_1, 2j_2)]$. Make the ansatz

$$Q_3(\rho_3) = (\rho_3 - s)^2(\rho_3 - t) = \rho_3^3 - (t + 2s)\rho_3^2 + (2st + s^2)\rho_3 - s^2t.$$

Comparing coefficients of the right most polynomial above with those of Q_3 (41) gives

$$t + 2s = 2(j_1 + j_2), \quad (42a)$$

$$2st + s^2 = 4j_1j_2, \quad (42b)$$

$$s^2 t = \frac{(j_1 + j_2 - h)^2}{\mu^2}. \quad (42c)$$

From (42c) it follows that $t \geq 0$. Taking the square root of both sides of this equation gives

$$j_1 + j_2 - h = \varepsilon_1 \mu s \sqrt{t}, \quad (43)$$

where $\varepsilon_1 = \pm$. Taking the difference of the squares of (42a) and four times (42b) gives

$$4(j_1 - j_2)^2 = t(t - 4s), \quad (44)$$

which implies that

$$\text{either } t \geq 4s \text{ and } t \geq 0 \text{ or } t = 0. \quad (45)$$

When either of the conditions (45) hold, we may take the square root of both sides of (44). We then obtain

$$2(j_1 - j_2) = \varepsilon_2 \sqrt{t(t - 4s)}, \quad (46)$$

where $\varepsilon_2 = \pm$. Adding and subtracting this from (42a) gives

$$j_1 = j_1(s, t) = \frac{1}{4}(t + 2s + \varepsilon_2 \sqrt{t(t - 4s)}), \quad j_2 = j_2(s, t) = \frac{1}{4}(t + 2s - \varepsilon_2 \sqrt{t(t - 4s)}). \quad (47)$$

Subtracting half of (42a) from (43) we obtain:

$$h = h(s, t) = \frac{1}{2}(t + 2s) - \varepsilon_1 \mu s \sqrt{t}. \quad (48)$$

Hence we have proved the following lemma.

Lemma 2. *Consider the mapping*

$$B_{\varepsilon_1, \varepsilon_2} : D \subseteq \mathbb{R}^2 \rightarrow \mathbb{R}^3 : (s, t) \mapsto (h(s, t), j_1(s, t), j_2(s, t)),$$

where D is the closed subset of \mathbb{R}^2 which is the union of: (1) the intersection of the closed half planes $\{s \geq 0\}$, $\{t \geq 0\}$, $\{t - 4s \geq 0\}$; and (2) the closed half line $L_- = \{(s, 0) \in \mathbb{R}^2 | s \geq 0\}$. For every choice of sign of ε_1 and ε_2 , the map $B_{\varepsilon_1, \varepsilon_2}$ parameterizes a patch of the set Σ . The image under $B_{\varepsilon_1, \varepsilon_2}$ of the closed half line L_+ is the thread:

$$\mathcal{T} = B_{\varepsilon_1, \varepsilon_2}(L_+) = \{(2j_1, j_1, j_1) \in \mathbb{R}^3 | j_1 \geq 0\},$$

which is attached to the two-dimensional pieces $B_{\varepsilon_1, \varepsilon_2}(D \setminus L_+)$ at the origin $(0, 0, 0)$.

Since the image of the energy momentum mapping \mathcal{EM} (40) is the closed region in \mathbb{R}^3 bounded by Σ and containing the thread \mathcal{T} , we see that the set of regular values given by the image minus Σ is *not* simply connected. Thus, the Liouville integrable system $(H, J_1, J_2, T^*\mathbb{R}^3, \omega)$ possibly has monodromy.

The set Σ of critical values of the \mathcal{EM} map is shown in Fig. 3. The points of the set Σ can be characterized as belonging to the three subsets introduced at the beginning of this section:

- (I) $j_1 \neq j_2 \neq 0$: these critical values correspond to the interior points of the four patches. The preimage under the energy momentum map \mathcal{EM} of each of these points is a two-torus in phase space. Their special feature is that since $\rho_3 = \text{const.}$ the instantaneous ellipse formed by their projection into the (x, y) -plane has constant eccentricity, see Section 7. In [7] they are referred to as elliptic–parabolic modes.

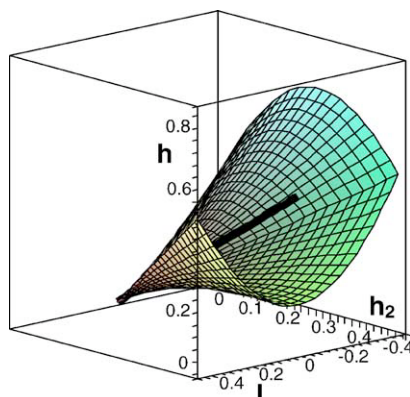


Fig. 3. Set of critical values Σ of the energy momentum map. It consists of two smooth patches intersecting in two lines and a thread \mathcal{T} (thick black line) connected to the former only at the origin. The image of the energy momentum map contains the thread, hence it is not simply connected.

- (II) $j_1 = j_2 \neq 0$: this condition determines the thread ($t = 0$, case IIa), and two lines in the smooth part of the boundary ($t = 4$ s, case IIb). Both cases imply that the angular momentum L vanishes and the energy of the quadratic terms H_2 satisfies $j_1 = j_2 = h_2/2$. For IIa we find $h = 2j_1 = h_2$; it represents the unstable springing motion including its separatrix. An ordinary tangency occurs for IIb and hence $h = h_2 - 2\varepsilon_1\mu(h_2/3)^{3/2}$. Unlike in case III here the preimage under \mathcal{EM} is a two-torus. However, each corresponding motion is periodic inside a plane through the z -axis. The union of all possible planar periodic orbits with fixed $(h, j_1 = j_2)$ gives a two-torus foliated by periodic orbits. In the planar two degree of freedom spring pendulum with vanishing angular momentum, case IIb corresponds to isolated periodic orbits, the cup ($\varepsilon_1 = +1$) and cap ($\varepsilon_1 = -1$) solutions, see [7,12].
- (III) $j_1 = 0$ or $j_2 = 0$: this condition describes the edges of Σ (those parameterized by $(s = 0)$), where two patches meet. These two curves in Σ represent the periodic orbits of left or right circular swinging motion (called conical motion in [7]). The angular momentum is maximal/minimal for fixed energy $h = \max(j_1, j_2)$ and each of the periodic orbits is a relative equilibrium. The point $j_1 = j_2 = 0$ is the equilibrium point at the origin of phase space.

All the remaining points in the image of \mathcal{EM} correspond to regular values and represent generic motion on three-tori. The set Σ has a nonlinear scaling symmetry, which will be used in later sections. By the usual convention l and h_2 denote the values of the conserved quantities L and H_2 , respectively. Our naming convention applied to the inverse of (23a) and (23b) gives

$$h_2 = j_1 + j_2, \quad l = j_2 - j_1. \quad (49)$$

We denote the scaled constants of motion by the corresponding Greek letters:

$$\chi = \frac{h - h_2}{\mu h_2^{3/2}}, \quad \lambda = \frac{l}{h_2}. \quad (50)$$

Scaling ρ_3 by h_2 gives a polynomial \tilde{Q}_3 (which replaces Q_3) that only depends on χ and λ , namely

$$\tilde{Q}_3(z) = z((1 - z)^2 - \lambda^2) - \chi^2. \quad (51)$$

By a calculation similar to the one that lead to Lemma 2 we find that

$$(\chi, \lambda) = (\varepsilon_1 s \sqrt{2 - 2s}, \varepsilon_2 \sqrt{(1 - 3s)(1 - s)}). \quad s \in [0, 1].$$

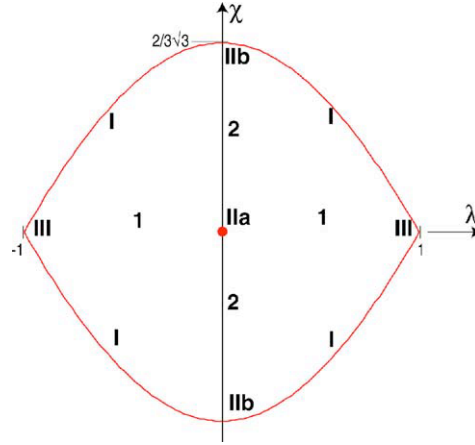


Fig. 4. The set Σ in scaled parameters (χ, λ) . The arabic numerals refer to the type of reduced phase space P_{j_1, j_2} . The roman numerals refer to the types of critical values of the energy momentum map. Topologically Fig. 3 is a cone over the set of critical values, with the same labeling.

So

$$\chi = \pm \frac{\sqrt{6}}{9} \sqrt{(1 + 3\lambda^2)^{3/2} - (1 - 9\lambda^2)}, \quad \lambda \in [-1, 1]. \quad (52)$$

The critical values give a lemon-shape in the (χ, λ) -plane shown in Fig. 4. The diagram in Fig. 4 is a section through the set of critical values Σ of the energy momentum map. The origin in the (χ, λ) -plane is the intersection with the thread, and gives an isolated singular point. Solving the definition of χ (50) for h , and then using (52) and $\lambda = (j_2 - j_1)/(j_2 + j_1)$ gives an explicit formula for the critical value h as a function of the momenta j_1 and j_2 .

7. Reconstruction: the swing plane angle

The most striking feature of the resonant swing spring is the phenomenon of stepwise precession of the swing plane. In Section 3, we have seen that the angle ϑ (15) gives the orientation of the ellipse in the xy -plane of the isotropic harmonic oscillator. For the full Hamiltonian H (21c) of the resonant swing spring we expect this ellipse to change orientation and eccentricity. However, its area is still constant, because the angular momentum L is conserved. When the solutions of the swing spring are projected to the xy -plane the geometry is similar to that of the harmonic oscillator. The functions ϑ (15) and κ (16) are defined in the same way as in Section 3 as functions of x, y, p_x, p_y , or ξ, η, p_ξ, p_η . Recall that for the 1:1 oscillator all the geometric characteristics of the projected orbits are determined by the invariants H_x, H_y, L , and M . All three such characteristics, orientation, eccentricity, and area are functions of the invariants, and hence are constant. For the swing spring each of these characteristics behave in a different way:

- *Area.* As before, the area of the (instantaneous) ellipse is given by πl^2 and is constant.
- *Eccentricity.* This is a function of κ (16); the difference between the swing spring and the harmonic oscillator is that

$$h_{xy} - l = \frac{1}{2}(x^2 + p_x^2 + y^2 + p_y^2) - (xp_y - yp_x) = \xi^2 + p_\xi^2 = \rho_1$$

is invariant under the two-torus symmetry group, but is not invariant under the Hamiltonian dynamics. For κ^4 we find

$$\kappa^4 = \frac{\xi^2 + p_\xi^2}{\eta^2 + p_\eta^2} = \frac{\rho_1}{\rho_2} = \frac{2j_1 - \rho_3}{2j_2 - \rho_3}, \quad (53)$$

which is a function of ρ_3 (which in general is nonconstant). For critical motion of type I, IIb, and III, ρ_3 is constant. In these cases the eccentricity is constant. For the most interesting case IIa, it is only constant on the hyperbolic orbit itself, but not on its separatrix.

- *Orientation.* The swing plane is defined by

$$\vartheta = \frac{1}{2} \left(\frac{\pi}{2} + \arg(\eta - ip_\eta) - \arg(\xi - ip_\xi) \right). \quad (54)$$

The difference with the harmonic oscillator is that ϑ cannot be expressed in terms of the invariants ρ_i of the two-torus symmetry group. Hence it is not a function of the reduced dynamics. Instead it is defined by a differential equation that is determined by and is driven by the reduced dynamics.

We want to compute the change of ϑ between one swinging phase and the next. Recall that ρ_3 is the energy in the z motion, that is, ρ_3 is the square of the amplitude of the motion in z direction. Therefore, we want to compute the change of ϑ over a complete period of the reduced motion of ρ_3 .

In the 1:1 oscillator, H_{xy} and L are integrals the motion. In the 1:1:2 resonant swing spring H_2 and L are instead. We prefer to use J_1, J_2 (23a) and (23b) and the conjugate angles θ_1, θ_2 (which are the difference and sum of the angles α and ϑ , see (14) and (15)). Excluding the cases where $\xi = p_\xi = 0$ or $\eta = p_\eta = 0$, we see that $(j_1, j_2, \theta_1, \theta_2)$ form a coordinate system for the motion on two-tori.

In Section 5, we have found a Hamiltonian 2-torus action (25) on $T^*\mathbb{R}^3$ with momentum map $\mathcal{J} = (J_1, J_2)$ (26). For a regular value (j_1, j_2) of \mathcal{J} , the two-torus action on the level set $\mathcal{J}^{-1}(j_1, j_2) = (J_1)^{-1}(j_1) \cap (J_2)^{-1}(j_2)$ is free. Hence we obtain a smooth 2-torus bundle $\pi_{j_1, j_2} : \mathcal{J}^{-1}(j_1, j_2) \rightarrow P_{j_1, j_2}$ over the reduced space P_{j_1, j_2} . We would like to find action-angle coordinates for this completely integrable system.

Lemma 3. *Outside the origin of the (ξ, p_ξ) -plane and the origin of the (η, p_η) -plane the functions $(j_1, \theta_1, j_2, \theta_2)$ given by*

$$\theta_1 = \arg(\xi - ip_\xi), \quad \theta_2 = \arg(\eta - ip_\eta) \quad (55)$$

and ρ_3, ρ_4, ρ_5 define a map from the phase space $T^*\mathbb{R}^3$ into the closed subset of $T^2 \times \mathbb{R}^2 \times \mathbb{R}^3$ (with coordinates $(\theta_1, \theta_2, J_1, J_2, \rho_3, \rho_4, \rho_5)$) defined by the equation $\rho_4^2 + \rho_5^2 = P_3(\rho_3)$ where P_3 is the cubic polynomial (33). In these coordinates, the Hamiltonian of the resonant swing spring is

$$H = J_1 + J_2 + \mu\rho_4. \quad (56)$$

Moreover, the following Poisson bracket relations hold:

$$\{\theta_1, J_1\} = 1, \quad \{\theta_2, J_2\} = 1, \quad (57a)$$

$$\{\theta_1, \rho_4\} = \frac{\rho_4}{\rho_1}, \quad \{\theta_1, \rho_5\} = \frac{\rho_5}{\rho_1}, \quad (57b)$$

$$\{\theta_2, \rho_4\} = \frac{\rho_4}{\rho_2}, \quad \{\theta_2, \rho_5\} = \frac{\rho_5}{\rho_2}, \quad (57c)$$

$$\{\rho_3, \rho_4\} = 2\rho_5, \quad \{\rho_3, \rho_5\} = -2\rho_4, \quad \{\rho_4, \rho_5\} = \rho_3(\rho_1 + \rho_2) - \rho_1\rho_2, \quad (57d)$$

where $\rho_1 = 2J_1 - \rho_3$, $\rho_2 = 2J_2 - \rho_3$ and all other brackets vanish.

Proof. The last assertion can be verified by direct calculation using the old variables $(\xi, \eta, \zeta, p_\xi, p_\eta, p_\zeta)$. The first statement is straightforward consequence of the fact that the functions ρ_i give an embedding of the reduced space, J_1, J_2 are the momenta of the reducing action and the angles θ_1, θ_2 are coordinates in the two-toric fibers of the reduction, as can be deduced by the commutation relations.

The fact that all brackets between the new variables can be expressed in terms of the ρ_i follows from the fact that the flow of the Hamiltonian vector fields of J_1 and J_2 leaves ρ_i -invariant and that the actions J_1 and J_2 and the angles θ_1, θ_2 form a symplectic coordinate system in the two-torus fiber of the bundle π_{j_1, j_2} . \square

Lemma 3 allows us to give a description of the motion of the resonant swing spring in phase space by decomposing it into a reduced system, which is an invariant subsystem that drives the dynamics in the fibers. Using the fact that $\mu\rho_4 = h - j_1 - j_2$, the equations of motion for the angles in a fiber are

$$\dot{\theta}_1 = \{\theta_1, H\} = 1 + \frac{h - j_1 - j_2}{\rho_1} = 1 + \frac{h - j_1 - j_2}{2j_1 - \rho_3}, \quad (58a)$$

$$\dot{\theta}_2 = \{\theta_2, H\} = 1 + \frac{h - j_1 - j_2}{\rho_2} = 1 + \frac{h - j_1 - j_2}{2j_2 - \rho_3}. \quad (58b)$$

They are driven by the solution of the second order differential equation:

$$\ddot{\rho}_3 = 2\mu^2 P'_3(\rho_3) = 2\mu^2((2j_1 - \rho_3)(2j_2 - \rho_3) - 2\rho_3(j_1 + j_2 - \rho_3)). \quad (59)$$

From Eqs. (58a) and (58b), one sees that the time derivative of the swing angle ϑ (15) satisfies

$$\dot{\vartheta} = \frac{1}{2}(\dot{\theta}_2 - \dot{\theta}_1) = \frac{(h - j_1 - j_2)(j_2 - j_1)}{(2j_1 - \rho_3)(2j_2 - \rho_3)} = \frac{(h - h_2)l}{(h_2 + l - \rho_3)(h_2 - l - \rho_3)}. \quad (60)$$

Both Eq. (59) and (60) can be found in [5]. We rederived them here because in [5] they were obtained under the hypothesis of “pattern evocation in shape space”, which might have been an approximation. From our derivation we see that *no* approximation is involved and that the angle of the swing plane is simply an angle of an action-angle coordinate system. The stepwise precession of the swing plane, that is, the change of ϑ over a complete period of ρ_3 , is independent of the initial angle ϑ . Integrating (60) gives the precession angle as an integral of a periodic function over the period of the function. Therefore, the stepwise precession angle is independent of the initial angle ϑ , and in particular is the same between any two successive swinging modes of an orbit. In Sections 8 and 9 we explicitly calculate the stepwise precession angle.

In order to interpret (60) it is best to eliminate ρ_3 and replace it by the eccentricity e . This is done in two steps. First ρ_3 is replaced by κ by simply solving (53). In the second step, κ is eliminated in favor of e using (16).⁵ This gives

$$\dot{\vartheta} = \frac{h - h_2}{l} \frac{1}{((\kappa^4 + 1)/(\kappa^4 - 1))^2 - 1} = 4 \frac{h - h_2}{l} \frac{1 - e^2}{e^4}. \quad (61)$$

This shows that ϑ is nearly constant when the swing spring is swinging, and hence $e \approx 1$, while ϑ changes very fast when the swing spring is springing, and hence $e \approx 0$. The fact that all the angle change occurs when it is impossible to see that the angle is changing (because the instantaneous ellipse is close to a circle) is the reason that makes the experimental observation so surprising and explains the stepwise nature of the precession.

Close to the homoclinic motion (separatrix of type IIa) with $j_1 \approx j_2$ and hence $l \approx 0$ and $h \approx h_2$ the z -energy ρ_3 sweeps out almost the whole range $[0, 2h_2]$. The largest eccentricity obtained is $\approx 1 - 2(l/h_2)^2$, which is close to 1, so that $\dot{\vartheta}$ is nearly zero, see Fig. 5.

⁵ The reason that the second step gives a rational function is that the expression is invariant under the replacement $\kappa \rightarrow 1/\kappa$, as e itself.

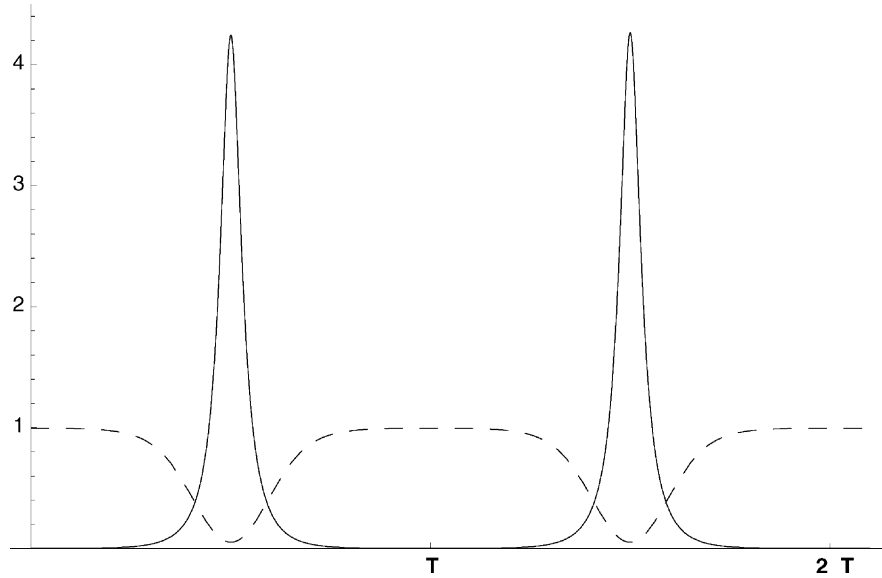


Fig. 5. The eccentricity $e(t)$ (dotted line) and the derivative of the swing-angle $\dot{\theta}(t)$ (solid line) for $j_1 = 1$, $j_2 = 1.1$, $h = 2.15$. When the eccentricity is about zero the rate of change of the swing-angle is maximal while, when the eccentricity is close to 1 the swing-angle is almost constant, see (61).

8. Monodromy and rotation numbers

Let us now compute the monodromy matrix for the swing spring system in a way similar to that used in [2]. As we have shown, the reduced system is everywhere periodic except for the homoclinic orbits (whose points are mapped onto the thread by the energy momentum map). To obtain an expression of the missing action function we will focus on the Θ_i , the change of θ_i over one period of the motion of ρ_3 . To do so we first express such change as the time integral of the time derivative of θ_i and then, by changing the time parameterization, we will obtain Θ_i as the integral of an elliptic differential of third kind.

Any integral curve in the reduced system is given by the h -level set of the reduced Hamiltonian H_{j_1, j_2} (56) on the reduced space P_{j_1, j_2} (32). Hence every motion takes place on a family of real elliptic curves:

$$\mathcal{E}_{h, j_1, j_2} = \left\{ (\rho_3, \rho_5) : \rho_5^2 = \rho_3(\rho_3 - 2j_1)(\rho_3 - 2j_2) - \frac{(h - j_1 - j_2)^2}{\mu^2} \right\}, \quad (62)$$

where $0 \leq \rho_3 \leq \min(2j_1, 2j_2)$. Eq. (62) is obtained by eliminating ρ_4 from (26) using the equation $H_{j_1, j_2} = h$ (preservation of energy) which becomes $h = j_1 + j_2 + \mu\rho_4$. This reproduces the polynomial Q_3 (41). Therefore, the analysis of the double roots of Q_3 which we did for the energy momentum map also applies here.

Eq. (59) can be integrated at once and we find

$$\dot{\rho}_3 = 2\mu\rho_5 = \pm 2\mu\sqrt{Q_3(\rho_3)}. \quad (63)$$

Note that (63) is the last of the reduced equations of motion (37). When (h, j_1, j_2) is a regular value of the energy momentum mapping \mathcal{EM} (40) of the swing spring (which we henceforth assume), the curve $\mathcal{E}_{h, j_1, j_2}$ (62) is smooth. When $h = j_1 + j_2$ the polynomial $P_3(\rho_3) = \rho_3(2j_1 - \rho_3)(2j_2 - \rho_3)$ is nonnegative on $[0, \min(2j_1, 2j_2)]$. Therefore the polynomial Q_3 has three *distinct* real roots:

$$0 \leq \rho_3^0 < \rho_3^- \leq \min(2j_1, 2j_2) \leq \max(2j_1, 2j_2) \leq \rho_3^+.$$

(With strict inequalities if $h \neq j_1 + j_2$.) The motion of the reduced system on $H_{j_1, j_2}^{-1}(h)$ takes place when ρ_3 lies in $[\rho_3^0, \rho_3^-]$. Since $H_{j_1, j_2}^{-1}(h)$ is diffeomorphic to a circle, as the reduced motion runs through a period, the time parameter ρ_3 traverses the interval $[\rho_3^0, \rho_3^-]$ forward and backward once. Accordingly the period of the driving motion (63) is given by

$$T = 2 \int_{\rho_3^0}^{\rho_3^-} \frac{d\rho_3}{2\mu\rho_5}. \quad (64)$$

The change of θ_i (58a) and (58b), $i = 1, 2$ over this period is

$$\Theta_i = \int_0^T \left(1 + \frac{h - j_1 - j_2}{\rho_i} \right) dt. \quad (65)$$

By a change of time scale using Eq. (63), the integral (65) becomes

$$\Theta_i = 2 \int_{\rho_3^0}^{\rho_3^-} \left(1 + \frac{h - j_1 - j_2}{\rho_i} \right) \frac{d\rho_3}{2\mu\rho_5}, \quad (66)$$

which is an integral along a closed loop of a differential form on $\mathcal{E}_{h, j_1, j_2}$. Denote by γ the loop encircling the points $(\rho_3^0, 0)$ and $(\rho_3^-, 0)$ in the complex plane and introduce the elliptic differentials:

$$\tau_0 = \frac{d\rho_3}{2\mu\rho_5}, \quad \tau_i = \frac{(h - j_1 - j_2) d\rho_3}{2(2j_i - \rho_3)\mu\rho_5}, \quad i = 1, 2.$$

The angle conjugate to ρ_3 advances by 2π in time T . The angle θ_i advances by Θ_i in that same time. Therefore, the rotation numbers W_i of the motion on a three-torus are given by the complete elliptic integrals:

$$-2\pi W_i(h, j_1, j_2) = \Theta_i = \oint_{\gamma} \tau_0 + \oint_{\gamma} \tau_i. \quad (67)$$

The first integral in (67) defines a smooth function for every regular value of \mathcal{EM} . The second gives a multi-valued function that, due to the residue of the pole in $(2j_i, 0)$, jumps 2π every time the parameters circle around the thread. The technique to prove this is identical to that used in [2].

To compute the jump of the rotation number W_1 one chooses a loop in the energy momentum domain that winds around the thread, say

$$t \mapsto (2j + \delta \sin t, j + \frac{1}{2}\delta \cos t, j - \frac{1}{2}\delta \cos t)$$

for δ sufficiently small, and then compute the values of the function I given by

$$\oint_{\gamma} \frac{\delta \sin t d\rho_3}{2(2j + \delta \cos t - \rho_3)\sqrt{\mu^2 \rho_3(2j + \delta \cos t - \rho_3)(2j - \delta \cos t - \rho_3) - \delta^2 \sin^2 t}}.$$

The above integral is not well defined when t equals π . In fact, for $t = \pi$ the pole of the differential coalesces with the branch point of the Riemann surface. To compute I as t tends to π from both sides one splits the path γ into the sum of two paths, as shown in Fig. 6. Therefore, the integral I can be written as

$$\oint_{\gamma} \tau_1 = \oint_{\gamma''} \tau_1 - \oint_{\gamma'} \tau_1. \quad (68)$$

The first integral in (68) defines a smooth function on a neighborhood of π ; while the second gives

$$\oint_{\gamma'} \tau_1 = \begin{cases} \pi & \text{if } t < \pi \\ -\pi & \text{if } t > \pi \end{cases}$$

The above computations prove the following proposition.

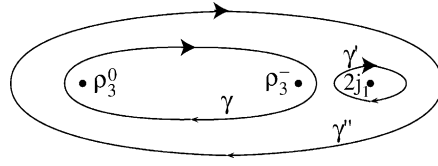


Fig. 6. The integration path γ in the complex ρ_3 -plane is equivalent to the path $\gamma'' - \gamma'$, where γ' encircles a pole of the differential.

Proposition 4. *The monodromy matrix of the swing spring, associated to the basis of $\pi_1(T^3)$ given by $\gamma_{J_1}(t) = \exp(tX_{J_1})$, $\gamma_{J_2}(t) = \exp(tX_{J_2})$ and*

$$\gamma_H(t) = \exp\left(\frac{t}{2\pi}(TX_H - \Theta_1 X_{J_1} - \Theta_2 X_{J_2})\right)$$

is the matrix

$$\begin{pmatrix} 1 & 0 & -1 \\ 0 & 1 & 1 \\ 0 & 0 & 1 \end{pmatrix}.$$

Also $\Theta = -2\pi W$, the change of the swing angle ϑ over one period of motion in the reduced space, is multi-valued with a jump equal to 2π . Hence, no matter how small the initial perturbation from the equilibrium is, one can always obtain all values of the rotation number W . In Section 9 we obtain an expansion of W in a neighborhood of the origin.

Now that the rotation numbers have been computed, we can explicitly obtain the third, multi-valued action for the system. The first two actions are the momenta of the 2-torus action J_1 and J_2 , they are single valued. The third is a function I_3 such that

$$dI_3 = \Theta_1(J_1, J_2, H) dJ_1 + \Theta_2(J_1, J_2, H) dJ_2 + T(J_1, J_2, H) dH. \tag{69}$$

dI_3 is a well defined local closed one-form, which can be integrated in a simply connected domain. From (69), we deduce that

$$dH = \frac{2\pi}{T(J_1, J_2, H)} dI_3 - \frac{\Theta_1(J_1, J_2, H)}{T(J_1, J_2, H)} dJ_1 - \frac{\Theta_2(J_1, J_2, H)}{T(J_1, J_2, H)} dJ_2 = \omega_3 dI_3 + \omega_1 dJ_1 + \omega_2 dJ_2. \tag{70}$$

The coefficients in front of the differentials of the local action functions are the *frequencies*. The ratio of the frequencies is a point in real projective two-space $\mathbb{R}P^3$ whose rationality degree is a characteristic of the invariant torus. In particular we re-obtain

$$W_i = \frac{\omega_i}{\omega_3} = -\frac{\Theta_i}{2\pi}.$$

9. Analysis of the swing angle

In this section, we examine more closely the change of the swing angle ϑ (54) over one period of the reduced motion. This is the stepwise precession angle:

$$2\pi W = -\Theta = -\frac{1}{2}(\Theta_2 - \Theta_1) = -\frac{1}{2} \oint_{\gamma} \tau_2 - \tau_1. \tag{71}$$

We prove the following proposition.

Proposition 5. *The rotation number describing the angle of stepwise precession for the integrable approximation of the resonant swing spring is given by*

$$2\pi W = -\arg(\chi + i\lambda) + O(\sqrt{\chi^2 + \lambda^2}). \quad (72)$$

Eq. (72) shows that the rotation number W is a multi-valued function of the parameters h , j_1 and j_2 . This therefore gives another proof of monodromy in the resonant swing spring.

Proof. In order to simplify the analytical study of (67) we remove an unneeded parameter by the rescaling (50)

$$\rho_3 = h_2 z, \quad l = h_2 \lambda \quad \text{and} \quad \frac{h - h_2}{\mu} = \chi h_2^{3/2}. \quad (73)$$

Eq. (71) then becomes

$$2\pi W = -\Theta = -\int_{z^0}^{z^-} \frac{\chi\lambda}{(1-z)^2 - \lambda^2} \frac{dz}{\sqrt{z((1-z)^2 - \lambda^2) - \chi^2}}. \quad (74)$$

Note that the polynomial under the square root is \tilde{Q}_3 (51). The distinct nonnegative roots of \tilde{Q}_3 are $0 \leq z^0 < z^- \leq 1 < z^+$.

Next we restrict the parameters χ and λ in (74) to lie on a line through the origin and assume that they are both small. In other words, we introduce a small parameter ε such that

$$\chi = \varepsilon a \quad \text{and} \quad \lambda = \varepsilon b, \quad (75)$$

where (a, b) are fixed in parameter space. Next we find the Taylor expansion of the roots z^0 , z^- , and z^+ in terms of the small parameter ε . A calculation gives

$$\begin{aligned} z^0 &= a^2 \varepsilon^2 + (2a^4 + a^2 b^2) \varepsilon^4 + O(\varepsilon^6), & z^- &= 1 - \sqrt{a^2 + b^2} \varepsilon - \frac{1}{2} a^2 \varepsilon^2 + O(\varepsilon^3), \\ z^+ &= 1 + \sqrt{a^2 + b^2} \varepsilon + \frac{1}{2} a^2 \varepsilon^2 + O(\varepsilon^3). \end{aligned} \quad (76)$$

Since the root z^- and the pole at $1 - \varepsilon b$ coalesce at 1 as $\varepsilon \rightarrow 0$, we introduce a shifted, scaled, and inverted new variable u by

$$z = 1 + \frac{\varepsilon b}{u}. \quad (77)$$

Inversion in the above formula ensures that the new integration limits are finite as $\varepsilon \rightarrow 0$. Denoting the transformed z^+ by u^+ etc., (74) becomes

$$2\pi\Theta = \int_{u^0}^{u^-} \frac{au^2}{u^2 - 1} \frac{du}{\sqrt{-u[(a^2 + b^2)u^3 - b^2u + \varepsilon b^3(u^2 - 1)]}}. \quad (78)$$

Now factor the polynomial under the square root as

$$-u[(a^2 + b^2)u^3 - b^2u + \varepsilon b^3(u^2 - 1)] = (u - u^0)(u^- - u)u(u - u^+)(a^2 + b^2)$$

and introduce a new integration variable φ by

$$2u = (u^- + u^0) + (u^- - u^0) \cos \varphi. \quad (79)$$

Then (78) becomes

$$2\pi\Theta = \frac{1}{\sqrt{a^2 + b^2}} \int_0^\pi f(u(\varphi)) \, d\varphi, \tag{80}$$

where

$$f(u) = \frac{au^2}{(u^2 - 1)\sqrt{u(u - u^+)}}. \tag{81}$$

Using (77) we find that (76) becomes

$$\begin{aligned} u^- &= -\frac{b}{\sqrt{a^2 + b^2}} - \frac{a^2 b}{a^2 + b^2} \varepsilon + O(\varepsilon^2), & u^0 &= -b\varepsilon + O(\varepsilon^3), \\ u^+ &= +\frac{b}{\sqrt{a^2 + b^2}} - \frac{a^2 b}{a^2 + b^2} \varepsilon + O(\varepsilon^2), \end{aligned} \tag{82}$$

which satisfy $u^- < u^0 < -\varepsilon b < 0 < u^+$ when $\varepsilon b > 0$. Expanding the integrand of (80) up through terms of order ε gives

$$\frac{-2ab(\cos \varphi - 1)^2}{(4a^2 + b^2(3 - \cos \varphi)(1 + \cos \varphi))\sqrt{(\cos \varphi - 1)(\cos \varphi - 3)}} + O(\varepsilon). \tag{83}$$

Note that the error term is uniformly bounded in the interval of integration. The main purpose of the above transformations was to achieve this.

Now the zeroth order contribution in (80) can be calculated. The substitution $\cos \varphi = 1 + 2 \sin \psi$ removes the root and the second substitution $\cos \beta = x$ rationalizes (83). Hence the integral becomes

$$\int_0^1 \frac{ab \, dx}{a^2 + b^2 x^2} = \tan^{-1} \frac{b}{a}. \tag{84}$$

Undoing the scaling gives the desired result. □

Using the above method, one can actually compute one more order. But it turns out to be zero. At $O(\varepsilon^2)$ the integrand is not uniformly bounded. So more sophisticated methods are needed to obtain the first nonzero correction. Note that the error term is small when we are close to the thread in the energy momentum domain. Then λ and χ are close to zero, see Fig. 4. Of course h_2 itself is also small, since we must be close to the equilibrium, but $\lambda = l/h_2$ and $\chi = (h - h_2)/(\mu h_2^{3/2})$ are assumed to be much smaller. The result means that for each fixed value of $h_2 > 0$, the swing angle Θ is a multi-valued function of l and h . This is an analytic proof that the system has monodromy. The resonant swing spring provides an example in which the monodromy can be easily observed.

Using these expansions of the roots of \tilde{Q}_3 we can also compute the range of the eccentricity for a motion near the thread. The result is

$$e \in \left[\frac{\chi^2}{\chi^2 + 2\lambda^2} + O(\varepsilon), 1 - 2\lambda^2 + O(\varepsilon^3) \right],$$

which shows that the ellipses always becomes close to lines, but not always close to a circle. This means that for all initial conditions with small χ and λ the swinging always takes place nearly inside a plane, which in fact is just a very elongated ellipse. However, we only find circles for the projected motion in the springing mode when the scaled energy difference χ is close to zero. This means that the amount of nonlinear energy $h - h_2$ in the motion is small. From (72) we see that the stepwise precession is close to $\pm\pi/2$. In the case of nearly linear motion, the

amount of scaled nonlinear energy χ in the motion is large compared to the scaled angular momentum λ . Then the minimal eccentricity never becomes close to 0, the motion always stays in a more or less eccentric ellipse, and $W \approx 0$. Intuitively one may say that with a nearly circular ellipse the swing plane changes easily, and hence W is large; while with an elongated nearly linear ellipse the swing plane does not change, and hence W is small.

Acknowledgements

This work was supported by the EU network HPRN-CT-2000-0113 *MASIE—Mechanics and Symmetry in Europe*. A first draft of this paper was written at University of Warwick during the Symposium on Geometric Mechanics and Symmetry 2002. The authors would like to thank the Math Research Center at Warwick for its hospitality. HRD was partially supported by EPSRC grant GR/R44911/01.

Appendix A

Proof of Lemma 1. By direct calculation it can be verified that α is conjugate to H_{xy} , that is, $\{\alpha, H_{xy}\} = 1$. To find the quadratic form satisfied by the ellipse E we use the integrals of the harmonic oscillator. Recall that (see [2]):

$$2H_x = x^2 + p_x^2, \quad M = xy + p_x p_y, \quad 2H_y = y^2 + p_y^2, \quad L = xp_y - yp_x \quad (\text{A.1})$$

are integrals of the two-dimensional harmonic oscillator vector field:

$$p_x \frac{\partial}{\partial x} + p_y \frac{\partial}{\partial y} - x \frac{\partial}{\partial p_x} - y \frac{\partial}{\partial p_y}. \quad (\text{A.2})$$

Moreover they satisfy the relation:

$$M^2 + L^2 = 4H_x H_y, \quad H_x \geq 0, \quad H_y \geq 0. \quad (\text{A.3})$$

The projection of a motion of the harmonic oscillator with initial condition (x^0, y^0, p_x^0, p_y^0) and positive energy onto the (x, y) -plane is the curve:

$$\gamma : t \mapsto \gamma(t) = (x(t), y(t)) = (x^0 \cos t + p_x^0 \sin t, y^0 \cos t + p_y^0 \sin t). \quad (\text{A.4})$$

The initial condition determines the values of the integrals, denoted by the corresponding small letter, and since they are constant in time we omit the superscript 0. Then

$$(2h_x - x(t)^2)(2h_y - y(t)^2) = (p_x(t)p_y(t))^2 = (m - x(t)y(t))^2,$$

which after some simplification gives

$$2h_y x(t)^2 - 2mx(t)y(t) + 2h_x y(t)^2 = 4h_x h_y - m^2 = l^2.$$

Since $h_x + h_y = h_{xy} > 0$ and $4h_x h_y - m^2 = l^2 \geq 0$, the quadratic form:

$$(x, y) \mathcal{Q} \begin{pmatrix} x \\ y \end{pmatrix} = (x, y) \begin{pmatrix} 2h_y & -m \\ -m & 2h_x \end{pmatrix} \begin{pmatrix} x \\ y \end{pmatrix} = l^2 \quad (\text{A.5})$$

is positive definite. Hence the curve γ (A.4) is an ellipse E . In complex coordinates $z = x + iy$ the quadratic form \mathcal{Q} reads

$$\frac{1}{2}(h_y - h_x + im)z^2 + (h_x + h_y)z\bar{z} + \frac{1}{2}(h_y - h_x - im)\bar{z}^2 = l^2. \quad (\text{A.6})$$

The form (A.6) is diagonal when the coefficients of z^2 and \bar{z}^2 are both real. Choosing ϑ so that $A := -(1/2)e^{2i\vartheta}(h_y - h_x + im)$ is real and positive, we see that the rotation $z = \zeta e^{i\vartheta}$ diagonalizes the form (A.6). We find

$$\begin{aligned} 2\vartheta &= -\arg(h_x - h_y - im) = \arg(x^2 + p_x^2 - y^2 - p_y^2 + 2i(xy + p_x p_y)) \\ &= \arg(p_\eta \xi - p_\xi \eta + i(\xi \eta + p_\xi p_\eta)) = \arg(i(\xi + ip_\xi)(\eta - ip_\eta)). \end{aligned} \quad (\text{A.7})$$

This proves (15).

In diagonal form (A.6) becomes $-\zeta^2 A + 2\zeta \bar{\zeta} B - \bar{\zeta}^2 A = l^2$, where $B = (1/2)(h_x + h_y)$. Since the coefficient $A \in \mathbb{R}$ and $A > 0$, we obtain

$$A = \frac{1}{2}(h_x - h_y - im)e^{2i\vartheta} = \frac{1}{2}|h_x - h_y + im| = \frac{1}{2}\sqrt{(h_x - h_y)^2 + m^2} = \frac{1}{2}\sqrt{(h_x + h_y)^2 - l^2}. \quad (\text{A.8})$$

Returning to real variables $\zeta = \xi + i\eta$ gives the diagonalized real quadratic form $2(B - A)\xi^2 + 2(B + A)\eta^2 = l^2$. Its semimajor axis a and semiminor axis b satisfy $1/a^2 = (B - A)/l^2$ and $1/b^2 = (B + A)/l^2$. Since $B > A$ (unless $l = 0$) it follows that $a > b$, as desired.

We now compute κ . By definition

$$\kappa^4 = \frac{h_x + h_y - l}{h_x + h_y + l} = \frac{2B - 2\sqrt{B^2 - A^2}}{2B + 2\sqrt{B^2 - A^2}} = \frac{(\sqrt{B + A} - \sqrt{B - A})^2}{(\sqrt{B + A} + \sqrt{B - A})^2}.$$

Extracting the square root gives

$$\kappa^2 = \frac{\sqrt{B + A} - \sqrt{B - A}}{\sqrt{B + A} + \sqrt{B - A}} = \frac{a - b}{a + b}. \quad (\text{A.9})$$

From this equation we find $b/a = (1 - \kappa^2)/(1 + \kappa^2)$. This together with the definition of the eccentricity gives

$$e^2 = 1 - \frac{b^2}{a^2} = \frac{4\kappa^2}{(1 + \kappa^2)^2}.$$

Extracting the square root gives the result. \square

References

- [1] V.I. Arnold (Ed.), *Dynamical Systems II*, Springer, Heidelberg, 1988.
- [2] R. Cushman, L. Bates, *Global Aspects of Classical Integrable Systems*, Birkhäuser, Basel, 1997.
- [3] J.J. Duistermaat, On global action angle coordinates, *Comm. Pure Appl. Math.* 33 (1980) 687–706.
- [4] S. Gutiérrez-Romero, J. Palacián, P. Yanguas, A universal procedure for normalizing N-DOF Hamiltonian systems, Preprint, 2003.
- [5] D.D. Holm, P. Lynch, Stepwise precession of the resonant swinging spring, *SIAM J. Appl. Dynam. Syst.* 1 (2002) 44–64.
- [6] P. Lynch, The swinging spring: a simple model for atmospheric balance, in: *Proceedings of the Symposium on the Mathematics of Atmosphere–Ocean Dynamics*, Isaac Newton Institute, June–December, 1996, Cambridge University Press, Cambridge.
- [7] P. Lynch, Resonant motions of the three-dimensional elastic pendulum, *Int. J. Nonlin. Mech.* 37 (2001) 345–367.
- [8] J.E. Marsden, J. Scheurle, Pattern evocation and geometric phases in mechanical systems with symmetry, *Dynam. Stabil. Syst.* 10 (1995) 315–338.
- [9] V. Matveev, Integrable Hamiltonian systems with two degrees of freedom, The topological structure of saturated neighborhoods of points of focus–focus and saddle–saddle type, *Sb. Math.* 187 (1996) 495–524.
- [10] N.N. Nehorošev, Action-angle variables, and their generalizations, *Trudy Moskov. Mat. Obšč.* 26 (1972) 181–198.
- [11] S. Vũ Ngọc, On semi-global invariants for focus–focus singularities, *Topology* 42 (2003) 365–380.
- [12] A. Vitt, G. Gorelik, Oscillations of an elastic pendulum as an example of the oscillations of two parametrically coupled linear systems (in Russian), *Zh. Tekh. Fiz.* 3 (1933) 294–307 (English translation by L. Shields, with an introduction by P. Lynch, Historical Note No. 3, Met Éireann, Dublin, 1999).
- [13] N.T. Zung, A note on focus–focus singularities, *Diff. Geom. Appl.* 7 (1997) 123–130.